Supplementary Information (SI)

Potential Lignin-Derived Alternatives to Bisphenol A in Diamine-Hardened Epoxy Resins

Kaleigh H. Nicastro,[†] Christopher J. Kloxin,[†, ‡, *] Thomas H. Epps, III[†, ‡, *]

[†]Department of Chemical & Biomolecular Engineering, University of Delaware, 150 Academy Street Newark, Delaware 19716, United States

[‡]Department of Materials Science & Engineering, University of Delaware, 127 The Green Newark, Delaware 19716, United States

*Corresponding Authors: (T.H.E.) thepps@udel.edu; (C.J.K.) cjk@udel.edu

Number of pages: 23

Number of schemes: 1

Number of tables: 4

Number of figures: 32

Proton (^{1}H) Nuclear Magnetic Resonance (NMR) spectrum for syringyl alcohol in deuterated chloroform ($CDCl_3$)

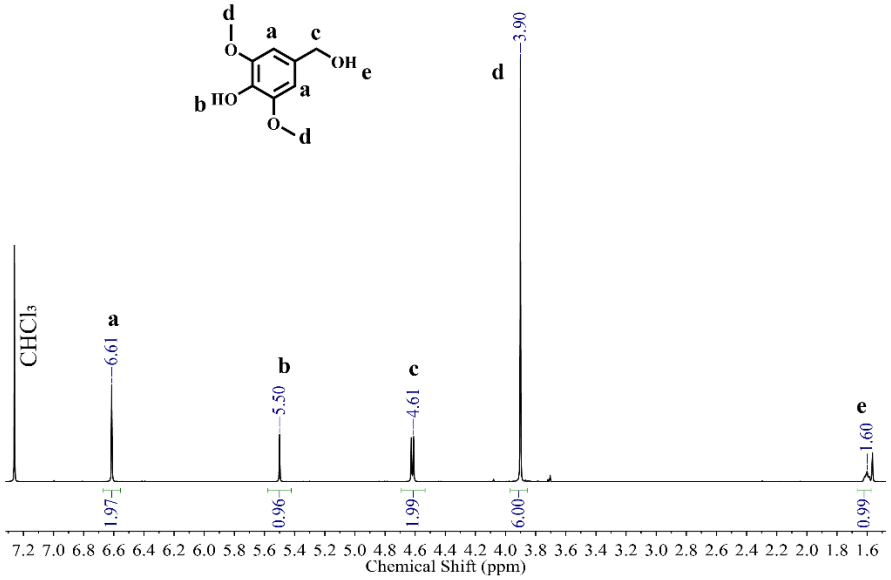

Figure S1. ^{1}H NMR spectrum of syringyl alcohol.

^{1}H, Carbon (^{13}C), ^{1}H-^{13}C Heteronuclear Single-Quantum Correlation (HSQC), and ^{1}H-^{13}C Heteronuclear Multiple-Bond Correlation (HMBC) NMR spectra for all bisguaiacols in $CDCl_3$

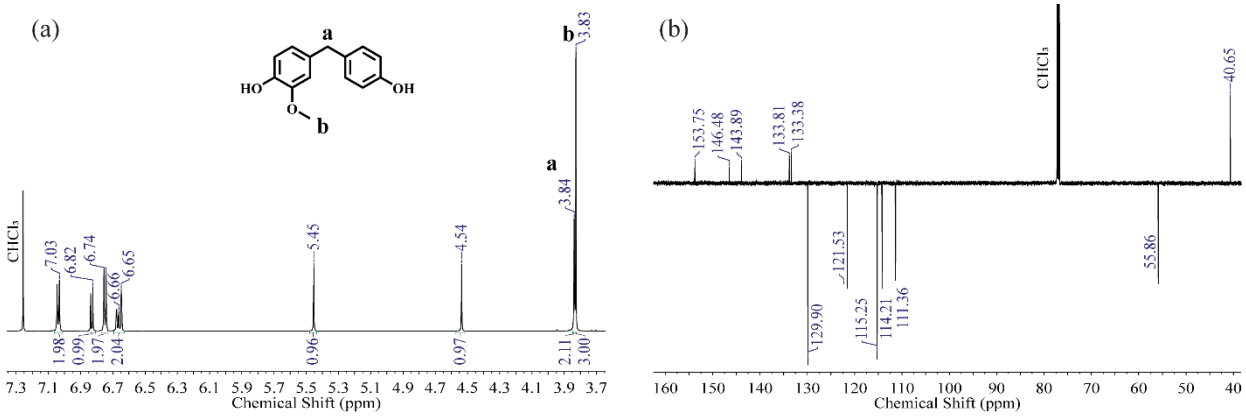

Figure S2. (a) ^{1}H NMR and (b) ^{13}C NMR spectra of *p,p'*-bisguaiacol P (BGP).

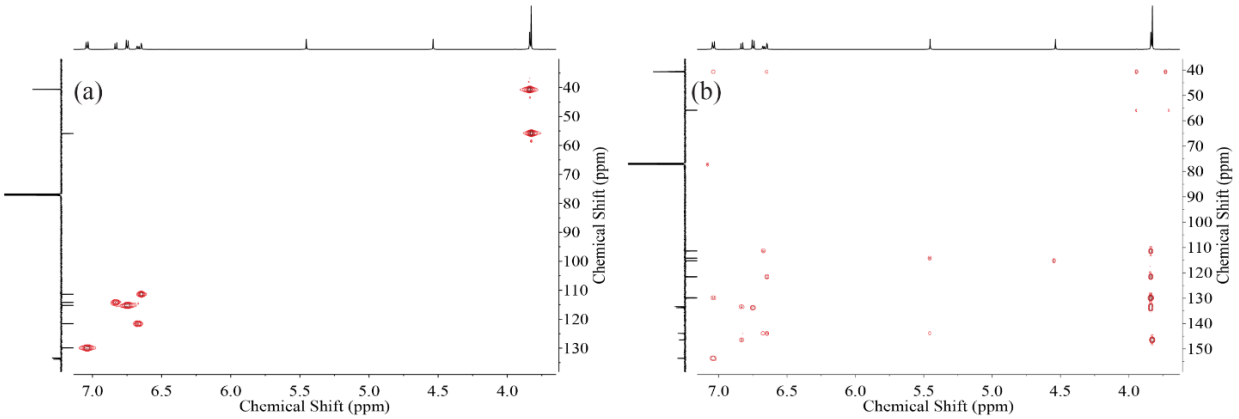

Figure S3. (a) HSQC and (b) HMBC NMR spectra of *p,p′*-BGP.

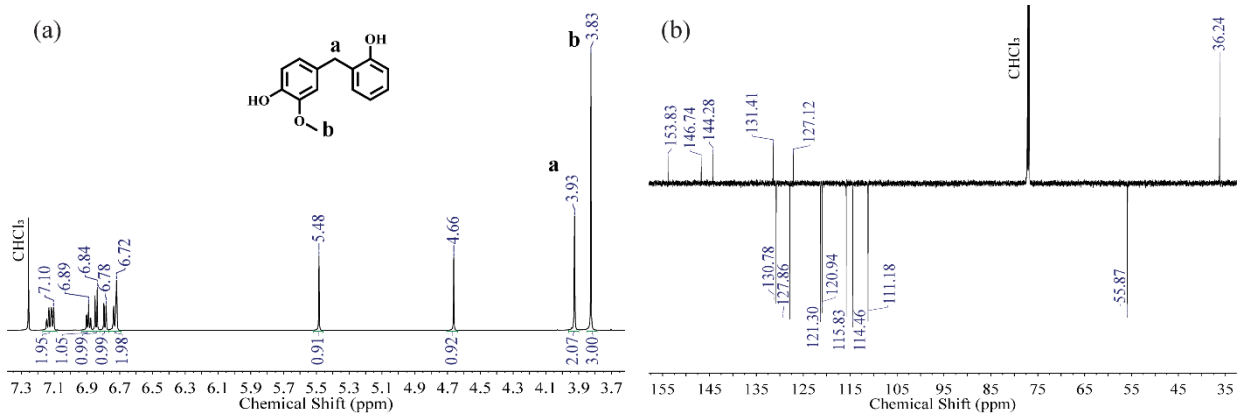

Figure S4. (a) ^{1}H NMR and (b) ^{13}C NMR spectra of *o,p′*-BGP.

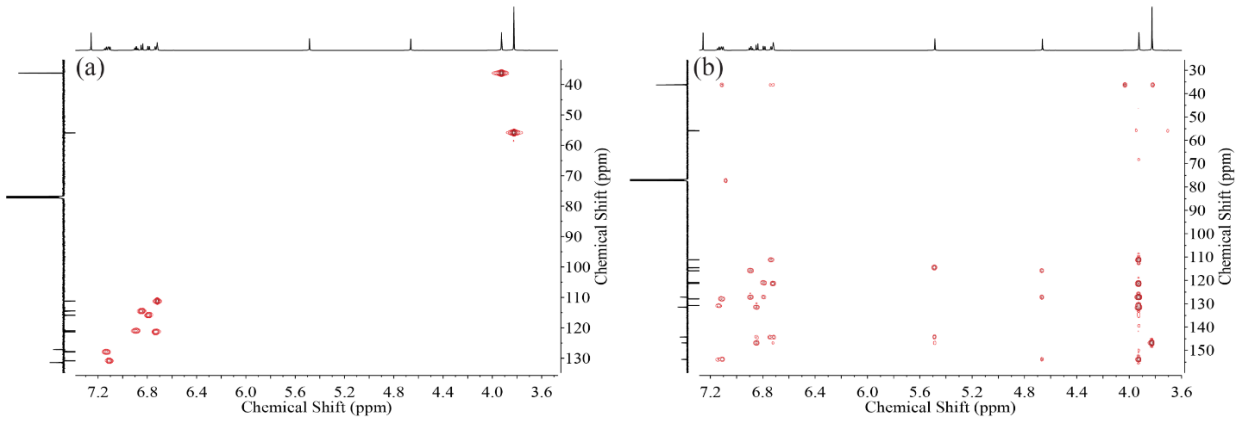

Figure S5. (a) HSQC and (b) HMBC NMR spectra of o,*p′*-BGP.

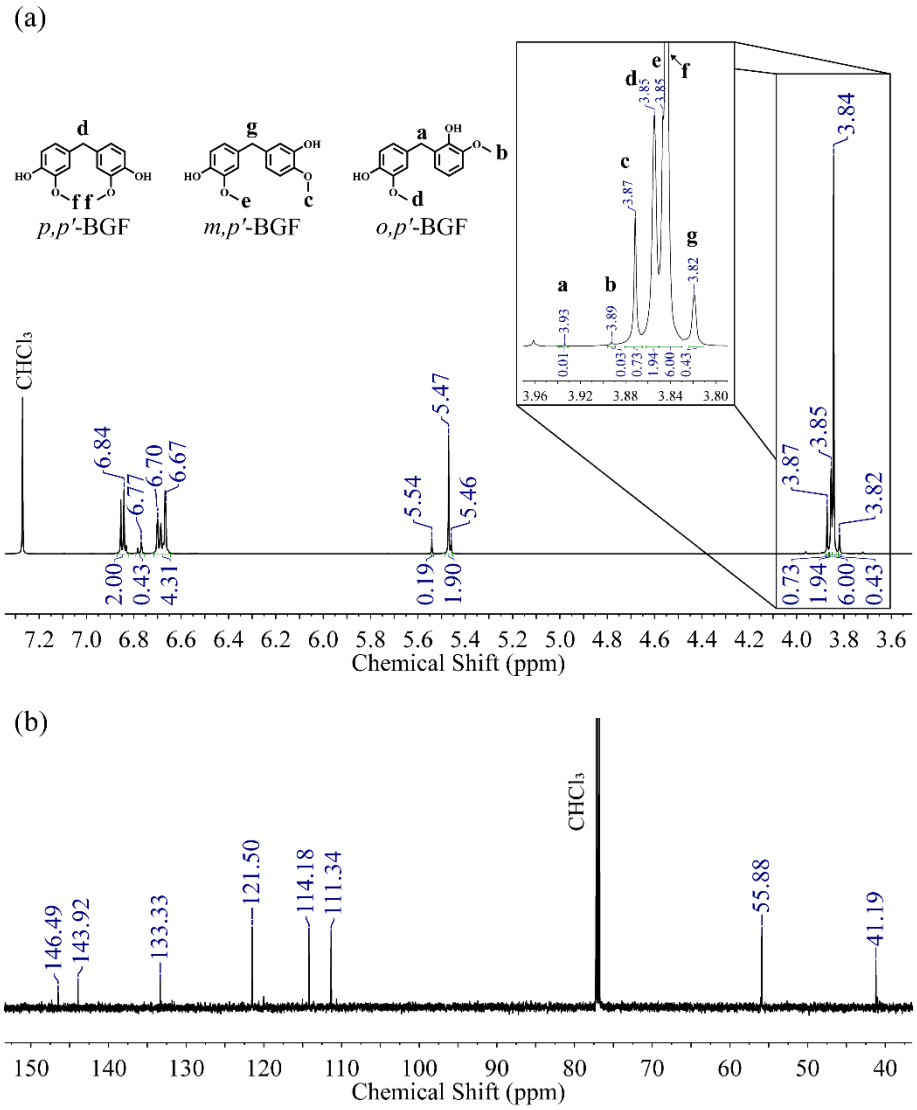

Figure S6. (a) ^{1}H NMR and (b) ^{13}C NMR spectra of bisguaiacol F (BGF).

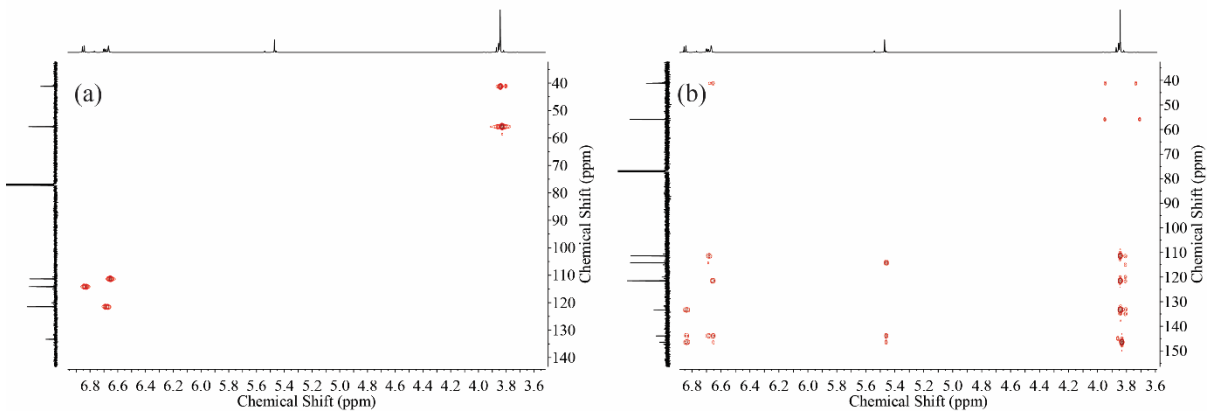

Figure S7. (a) HSQC and (b) HMBC NMR spectra of BGF.

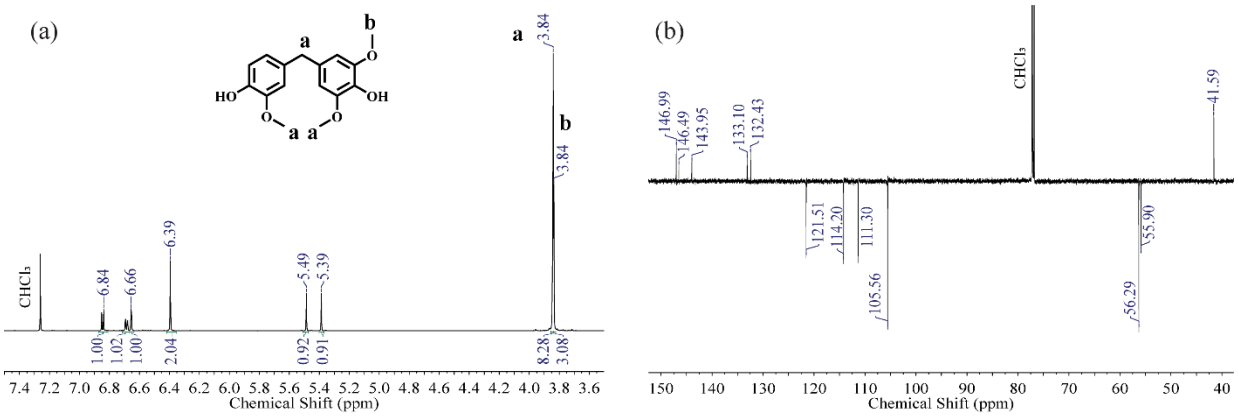

Figure S8. (a) ^{1}H NMR and (b) ^{13}C NMR spectra of *p,p′*-bisguaiacol S (BGS).

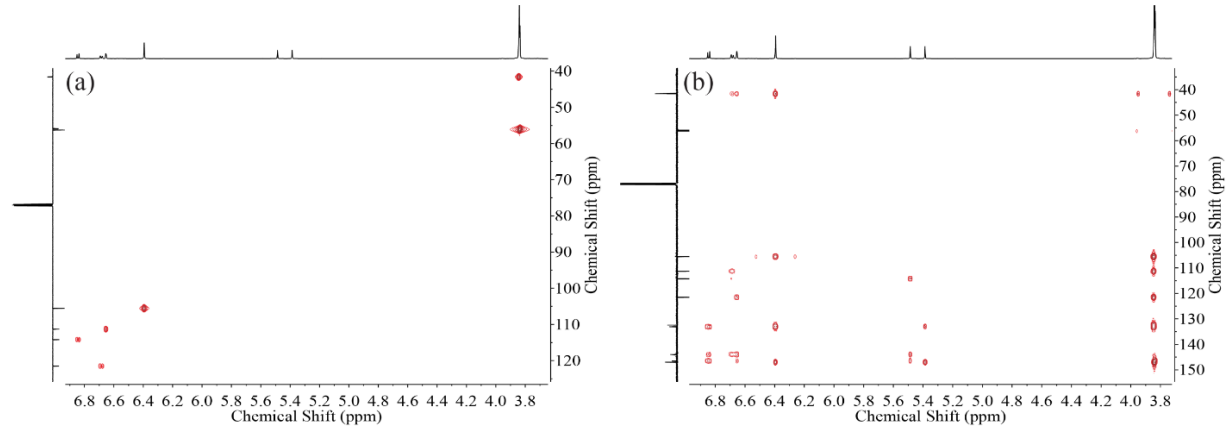

Figure S9. (a) HSQC and (b) HMBC NMR spectra of *p,p′*-BGS.

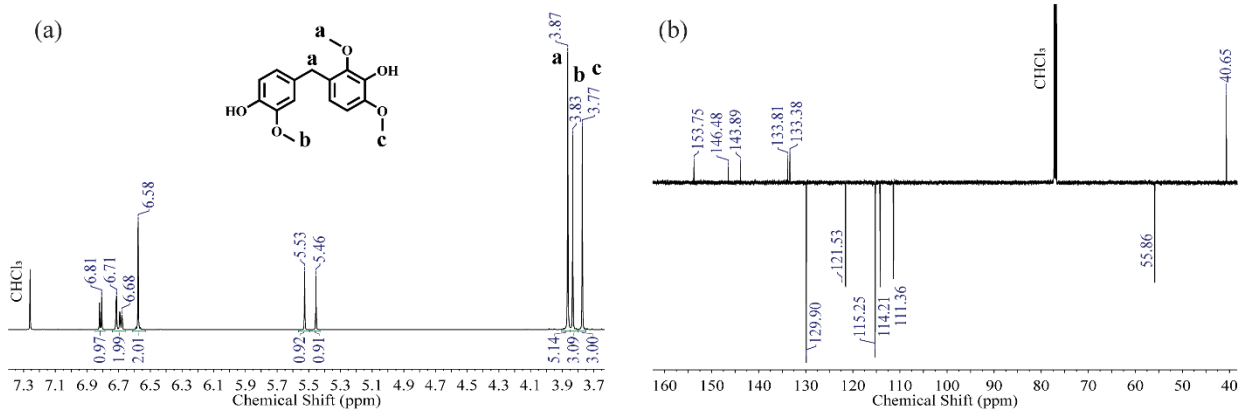

Figure S10. (a) ^{1}H NMR and (b) ^{13}C NMR spectra of *m,p′*-BGS.

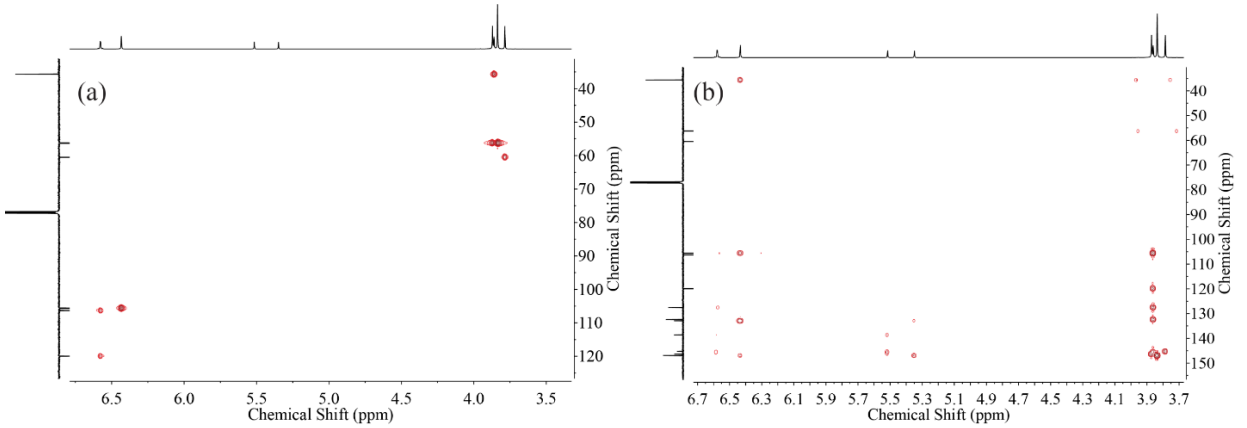

Figure S11. (a) HSQC and (b) HMBC NMR spectra of *m,p′*-BGS.

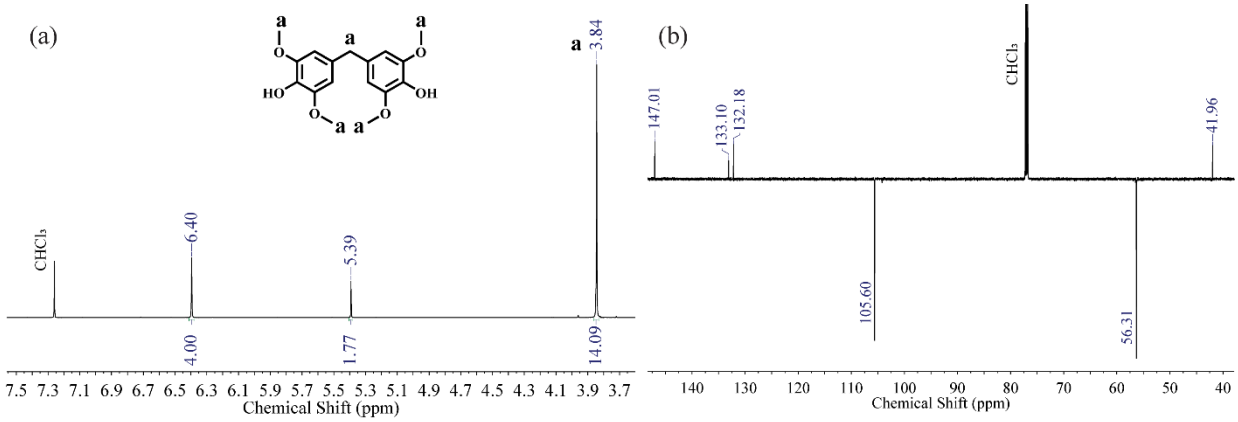

Figure S12. (a) ^{1}H NMR and (b) ^{13}C NMR spectra of *p,p′*-bisguaiacol M (BGM).

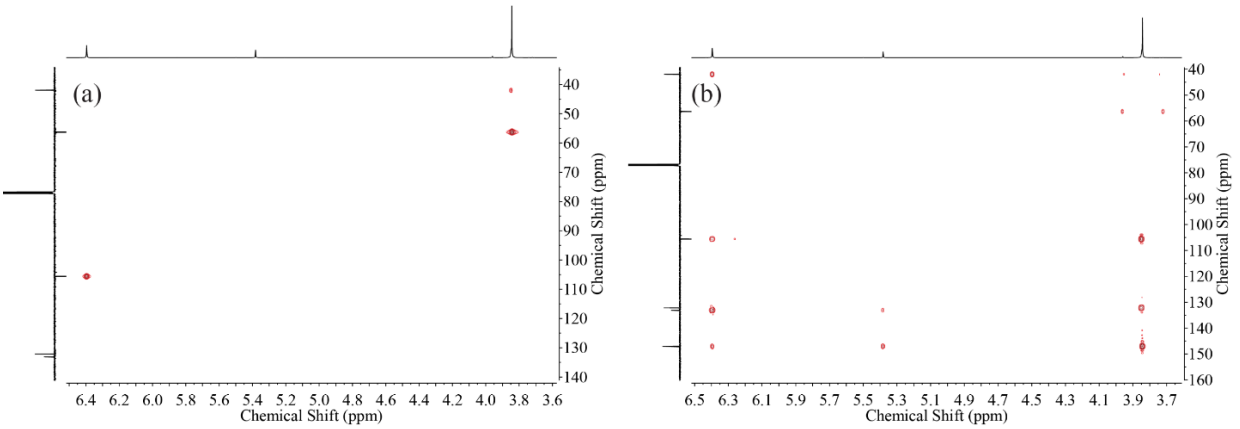

Figure S13. (a) HSQC and (b) HMBC NMR spectra of *p,p′*-BGM.

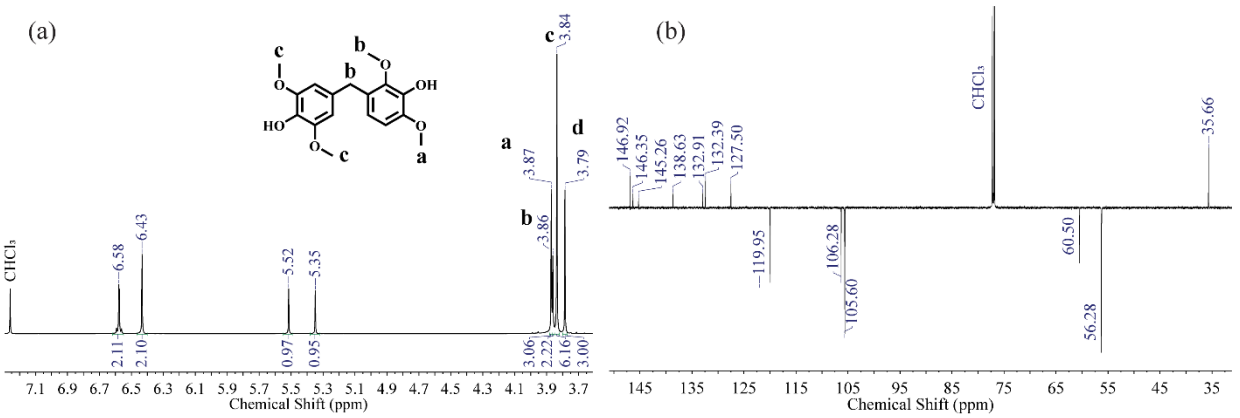

Figure S14. (a) ^{1}H NMR and (b) ^{13}C NMR spectra of *m,p′*-BGM.

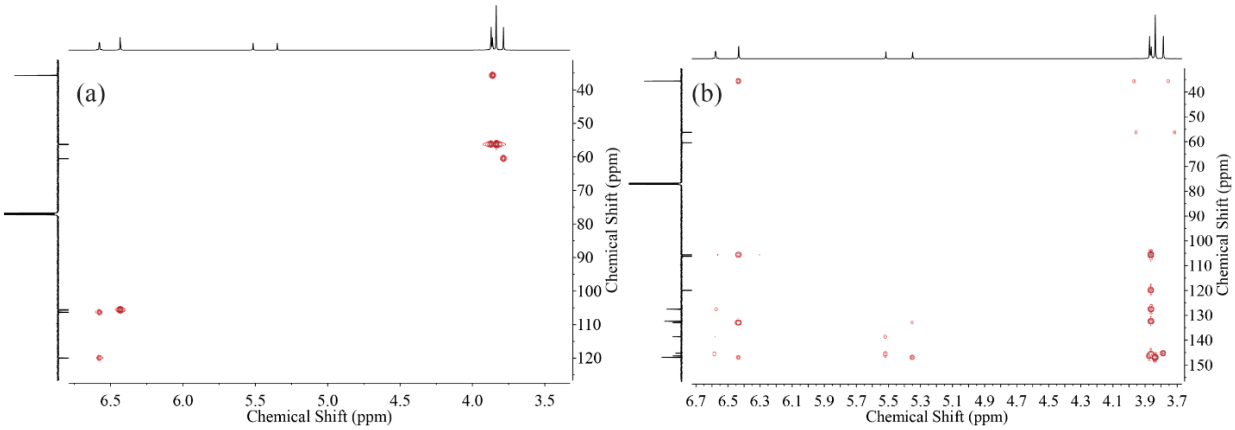

Figure S15. (a) HSQC and (b) HMBC NMR spectra of *m,p′*-BGM.

Table S1. Summary of bisguaiacols, BPA, and BPF melting points (T_m)s

Sample	T_m (°C)[a]
p,p′-BGP	122
o,p′-BGP	108
BGF	88
p,p′-BGS	95
m,p′-BGS	81
p,p′-BGM	104
m,p′-BGM	119
BPA	158
BPF	162

[a]Determined by differential scanning calorimetry (DSC) at a heating rate of 10 °C/min.

^{1}H NMR and ^{13}C NMR spectra for bisguaiacol diglycidyl ethers and the ^{1}H NMR spectra of bisphenol A diglycidyl ether (BADGE) and bisphenol F diglycidyl ether (BFDGE) in $CDCl_3$

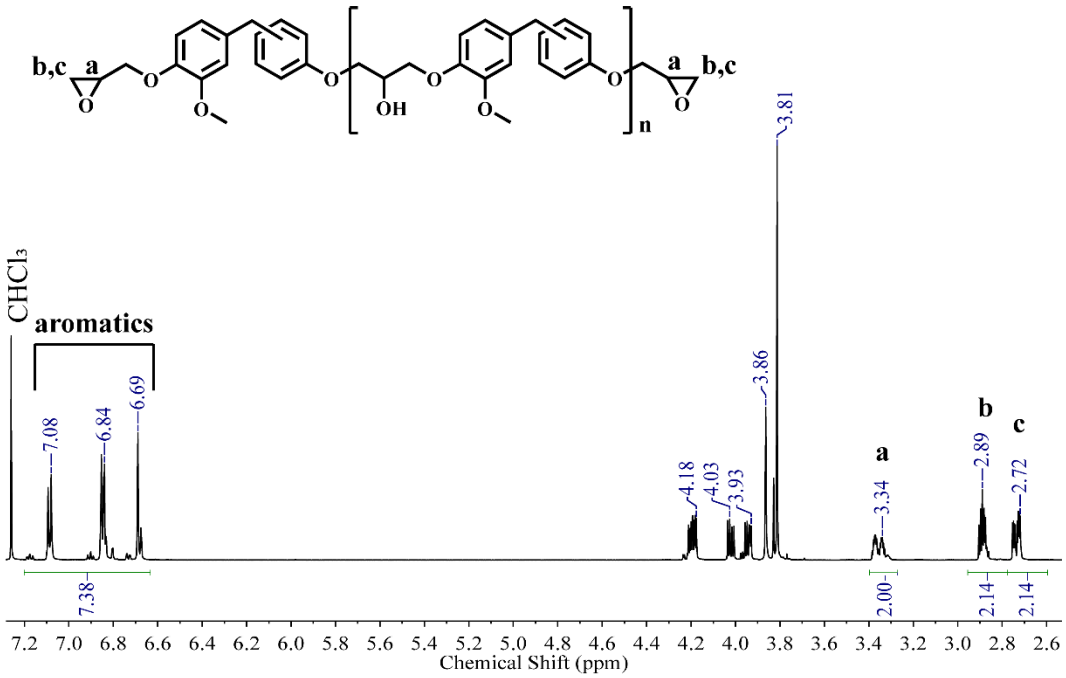

Figure S16. ^{1}H NMR spectrum of *mix*-bisguaiacol P diglycidyl ether (*mix*-BGPDGE) with peak assignments used to determine the extent of oligomerization (*n* value) and epoxy equivalent weight (EEW).

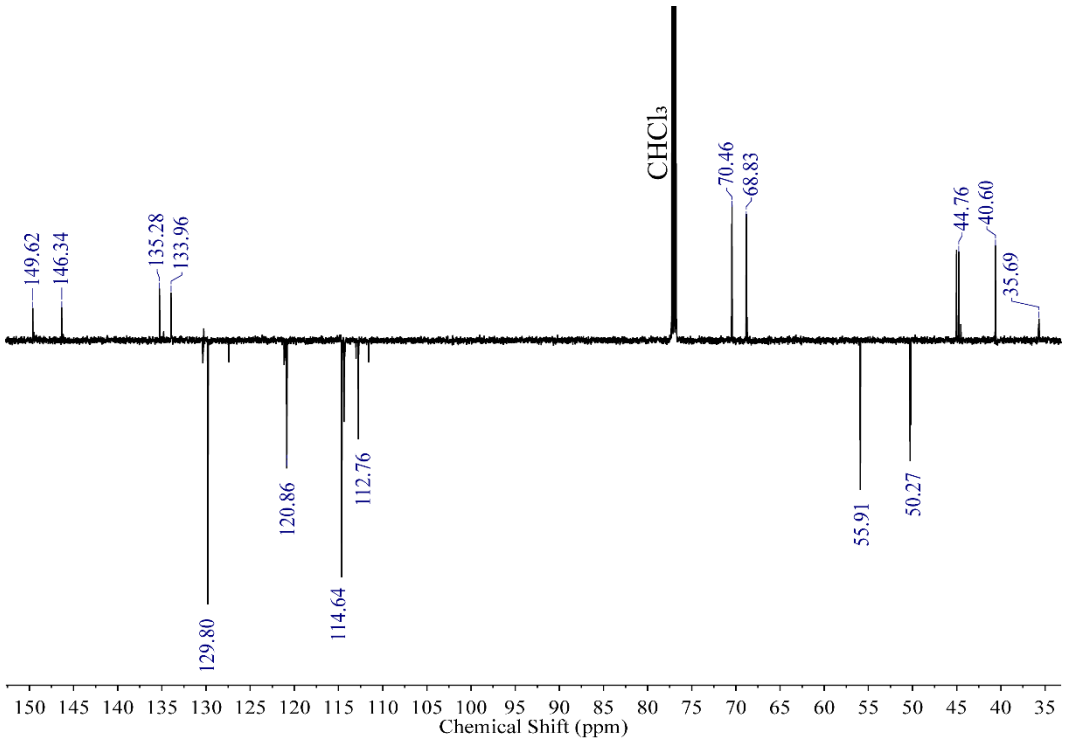

Figure S17. ^{13}C NMR spectrum of *mix*-BGPDGE.

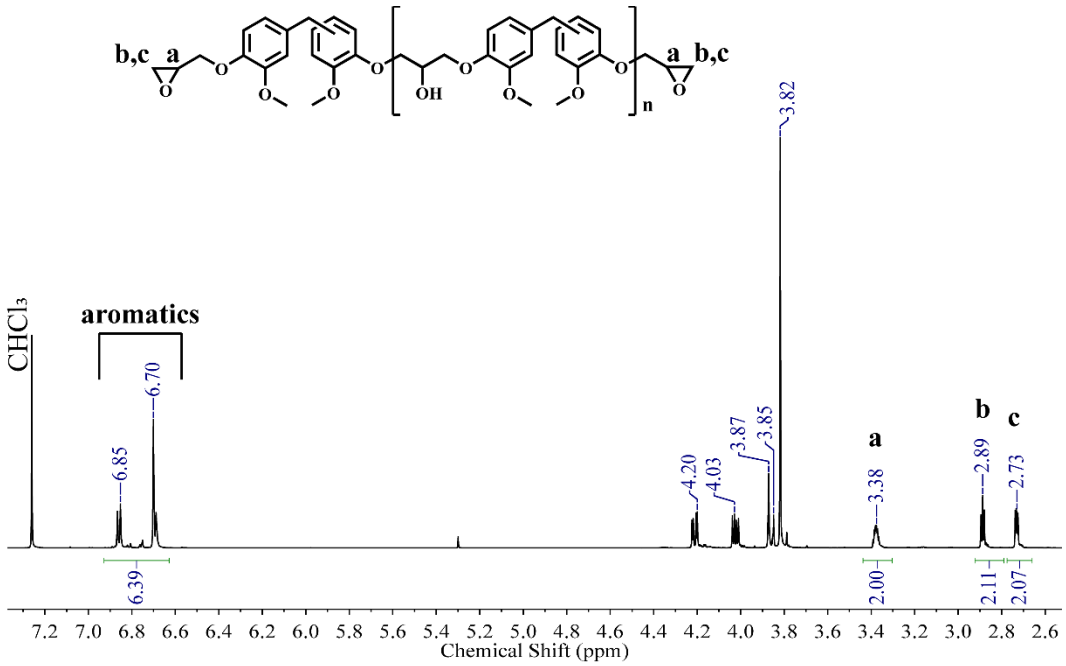

Figure S18. [1]H NMR spectrum of *mix*-bisguaiacol F diglycidyl ether (*mix*-BGFDGE) with peak assignments used to determine the *n* value and EEW.

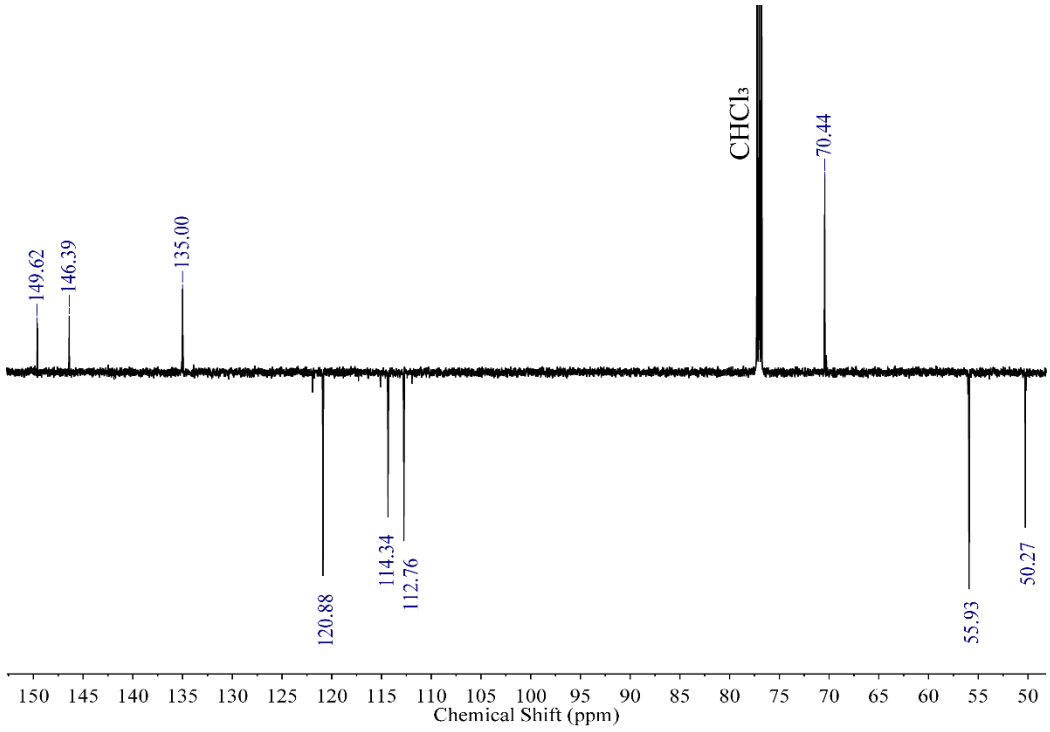

Figure S19. [13]C NMR spectrum of *mix*-BGFDGE.

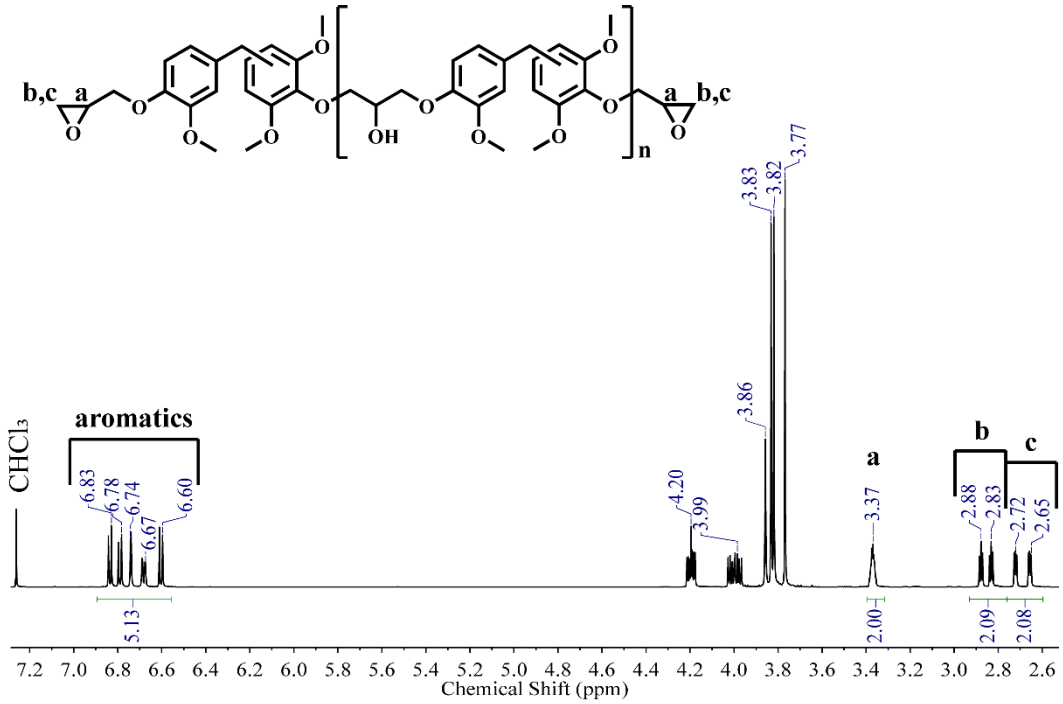

Figure S20. [1]H NMR spectrum of *mix*-bisguaiacol S diglycidyl ether (*mix*-BGSDGE) with peak assignments used to determine the *n* value and EEW.

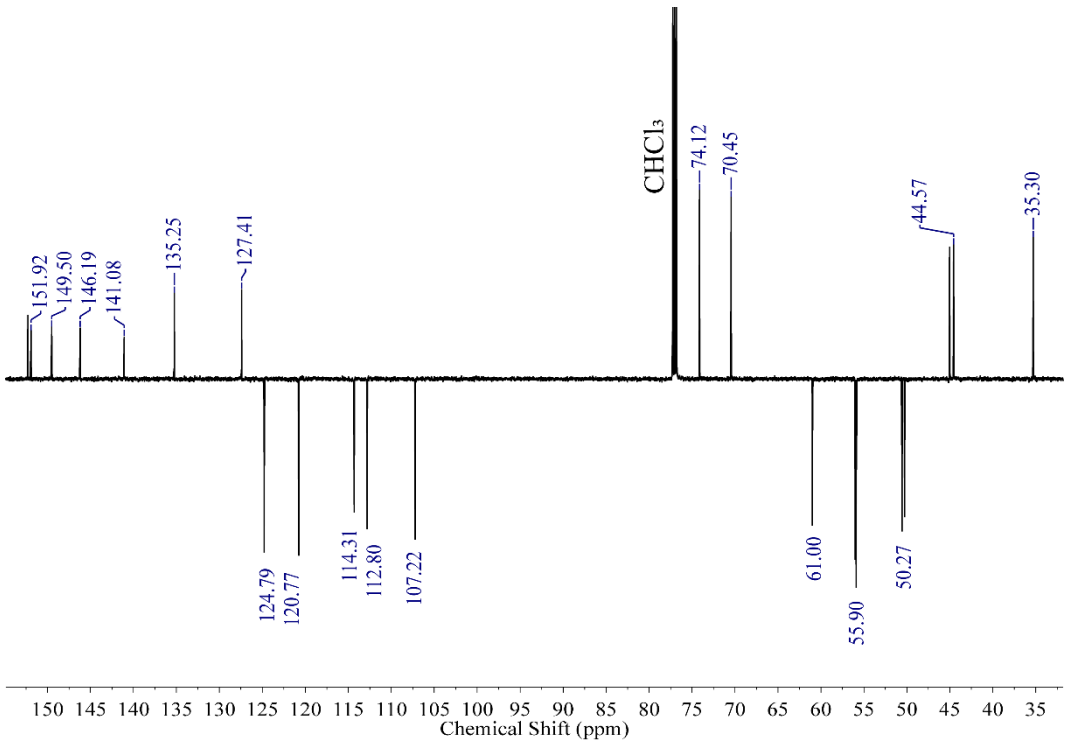

Figure S21. [13]C NMR spectrum of *mix*-BGSDGE.

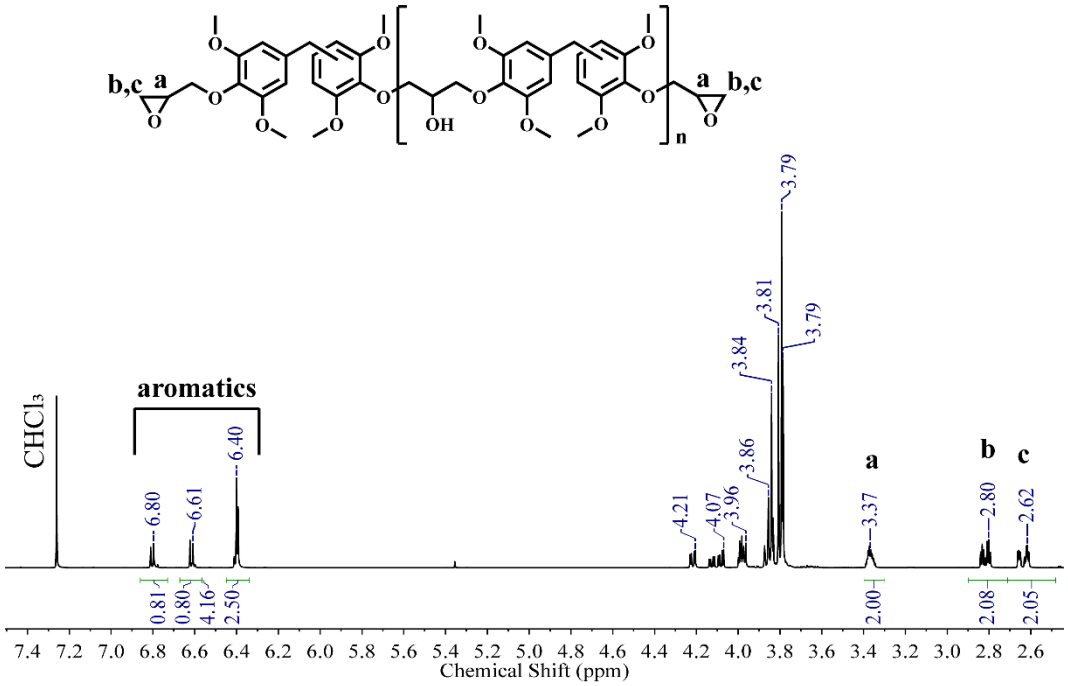

Figure S22. [1]H NMR spectrum of *mix*-bisguaiacol M diglycidyl ether (*mix*-BGMDGE) with peak assignments used to determine the *n* value and EEW.

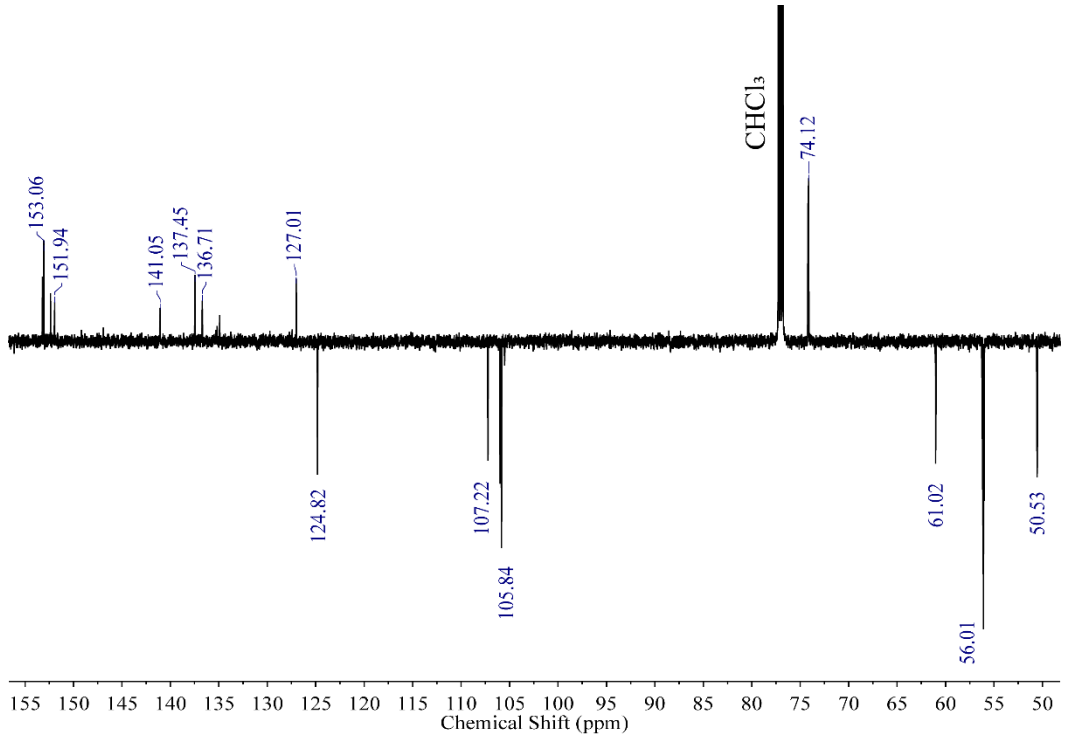

Figure S23. [13]C NMR spectrum of *mix*-BGMDGE.

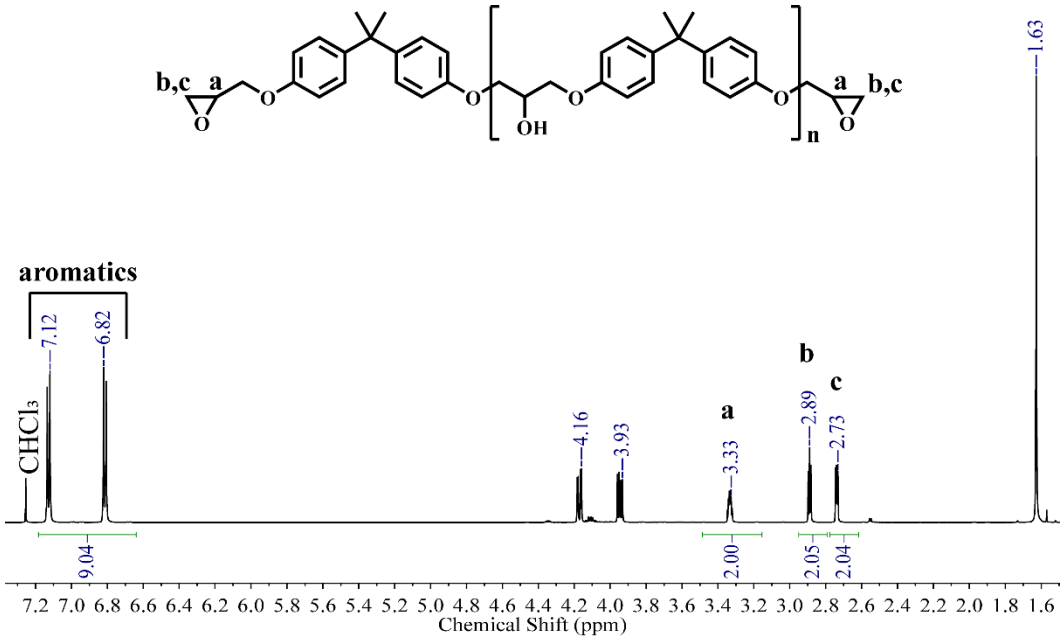

Figure S24. [1]H NMR spectrum of BADGE with peak assignments used to determine the *n* value and EEW.

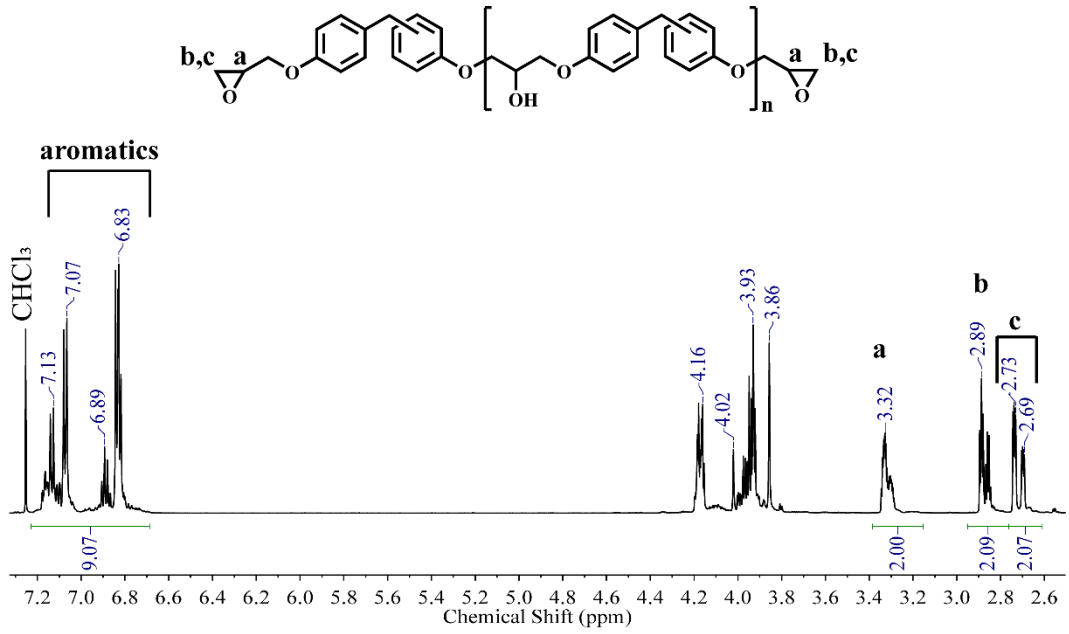

Figure S25. [1]H NMR spectrum of BFDGE with peak assignments used to determine the *n* value and EEW.

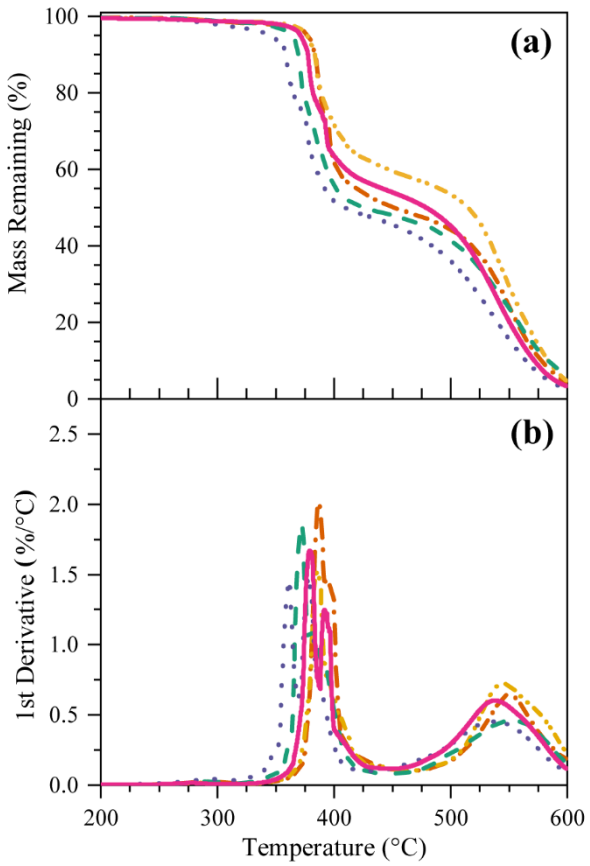

Figure S26. Thermogravimetric analysis (TGA) of MDA cured *mix*-BGPDGE (———), *mix*-BGSDGE (– – –), *mix*-BGMDGE (- - - -), BADGE (—·—), and BFDGE (—··—). (a) Sample mass remaining (%) as a function of temperature (b) and the first derivative of the sample mass remaining (%/°C) with respect to temperature in air (50 mL/min) at a heating rate of 10 °C/min.

Table S2. Temperature at which 5 wt% ($T_{5\%}$) of material was lost as determined by TGA for MDA cured diglycidyl ether samples in air (50 mL/min) at a heating rate of 10 °C/min.

Sample	$T_{5\%}$ (°C)
mix-BGPDGE	371
mix-BGSDGE	362
mix-BGMDGE	344
BADGE	378
BFDGE	376

Gel permeation chromatography (GPC)

Diglycidyl ether *n* values were confirmed through GPC analysis on a Viscotek VE2001 instrument with 7.8 × 300 mm Waters Styragel HR1and HR4 columns in series and tetrahydrofuran (THF, Optima) as the eluent (1.0 mL/min). Samples were injected at a diglycidyl ether concentration of 0.5 mg/mL in THF.

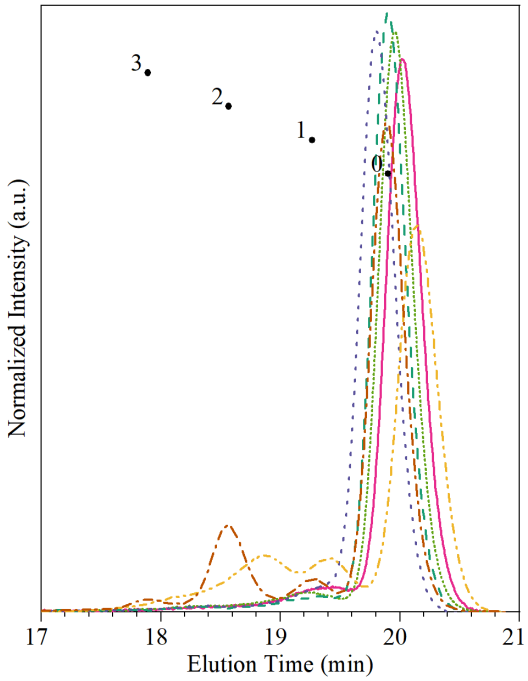

Figure S27. GPC traces of *mix*-BGPDGE (———), *mix*-BGFDGE (.....), *mix*-BGSDGE (– – –), *mix*-BGMDGE (- - - -), BADGE (—·—·), and BFDGE (—··—) relative to a BADGE standard (•) with varying *n* values (0–3) as a function of elution time. Molecular weights for the BADGE standard from 0 to 3 are 340, 625, 909, and 1193 g/mol, respectively.

Sample preparation for nonisothermal *in situ* curing studies using DSC

All diglycidyl ether samples, except *mix*-BGFDGE and *mix*-BGMDGE samples, were prepared by placing the diglycidyl ether and 4,4′-methylenedianiline (MDA) in a 2:1 diglycidyl ether:MDA molar ratio in a 10 mL polypropylene SpeedMixer™ plastic cup. The plastic cups were placed in an 80 °C oven for 6 min to melt all components and then immediately mixed in a SpeedMixer™ (DAC 150.1 FVZ-K, FlackTek, Inc.) for 3 min at 3000 rpm, sealed, and cooled to 0 °C until analysis to prevent premature curing. For BGFDGE and BGMDGE samples, solution mixing was employed. *mix*-BGFDGE, or *mix*-BGMDGE, and MDA were added to 20 mL glass scintillation vials in a 2:1 bisguaiacol diglycidyl ether:MDA molar ratio and dissolved in 1–2 mL of dichloromethane (DCM). The DCM was removed under reduced pressure, and the process was repeated once more to ensure homogenous mixing. The samples were dried under vacuum overnight, and the removal of DCM was confirmed by ^{1}H NMR spectroscopy.

DSC - curing studies

The reaction of diglycidyl ethers with MDA under nonisothermal curing conditions was studied using a DSC 214 Polyma (Neztsch) instrument. Prepared samples were loaded into pierced aluminum pans and cooled to 10 °C in the DSC under continuous nitrogen (N_2) flow (50 mL/min). Then, the samples were heated from 10 °C to 315 °C at a constant heating rate of 5 °C/min. Heats of reaction (H_R)s as a function of mmol of diglycidyl ether present in the resin mixture and conversions as a function of time were calculated using an approach outlined in the literature.[1, 2]

Table S3. H_R for the reaction of diglycidyl ethers with MDA determined by *in situ* DSC curing.

Sample	H_R (J/mmol diglycidyl ether)
mix-BGPDGE	247
mix-BGSDGE	237
mix-BGMDGE	184
BADGE	256
BFDGE	223

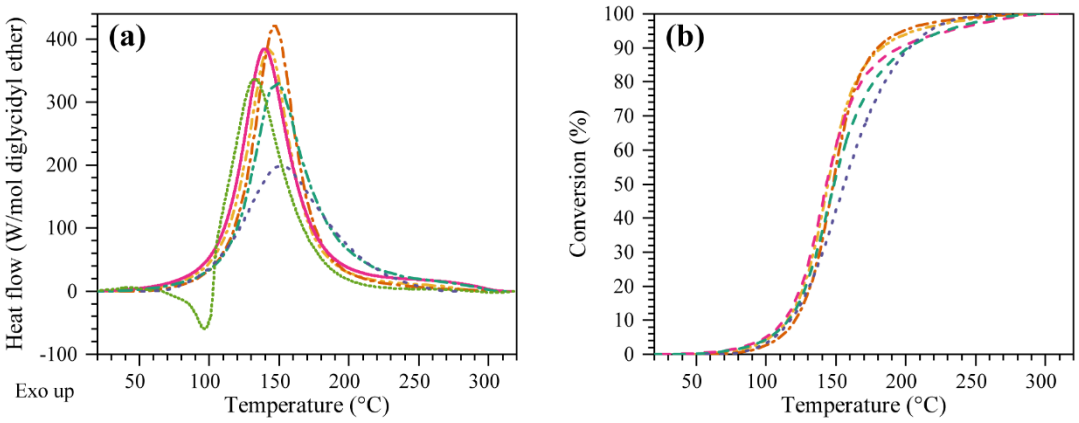

Figure S28. *In situ* (a) nonisothermal DSC exotherms and (b) epoxy conversion as a function of temperature for *mix*-BGPDGE (———), *mix*-BGFDGE (.....), *mix*-BGSDGE (– – –), *mix*-BGMDGE (- - - -), BADGE (–·–·–), and BFDGE (–··–) cured with MDA at a 2:1 molar ratio at a heating rate of 5 °C/min. All diglycidyl ethers exhibited autocatalytic nonisothermal curing, which is characteristic of epoxy-amine reactions. The conversion of BGFDGE was not determined because the curing exotherm was obscured by the melting endotherm of the reactants at 97 °C.

Fourier Transform Infrared Spectroscopy (FTIR)

A Nicolet IS50 Series FTIR spectrometer using a DTGS KBr detector was used to collect near IR spectra at room temperature. Final spectra were averaged over 16 scans. Background spectra of the glass slides were taken before loading samples and were subtracted from all spectra. Homogenous samples of individual diglycidyl ethers and MDA were prepared using the methods described above for DMA and TGA testing. Unreacted samples were placed between two glass slides separated by a 0.1 mm spacer. Initial spectra of samples were acquired before curing; then subsequent spectra were taken after curing. Near full conversion of MDA cured diglycidyl ethers was qualitatively confirmed using near FTIR by the disappearance of three principal peaks: the oxirane (i.e., epoxy) stretching second overtone peak at 4530 cm^{-1}, the overtone of the primary N-H bond at 5056 cm^{-1}, and the overtones of the primary and secondary N-H bond at 6670 cm^{-1}.[3]

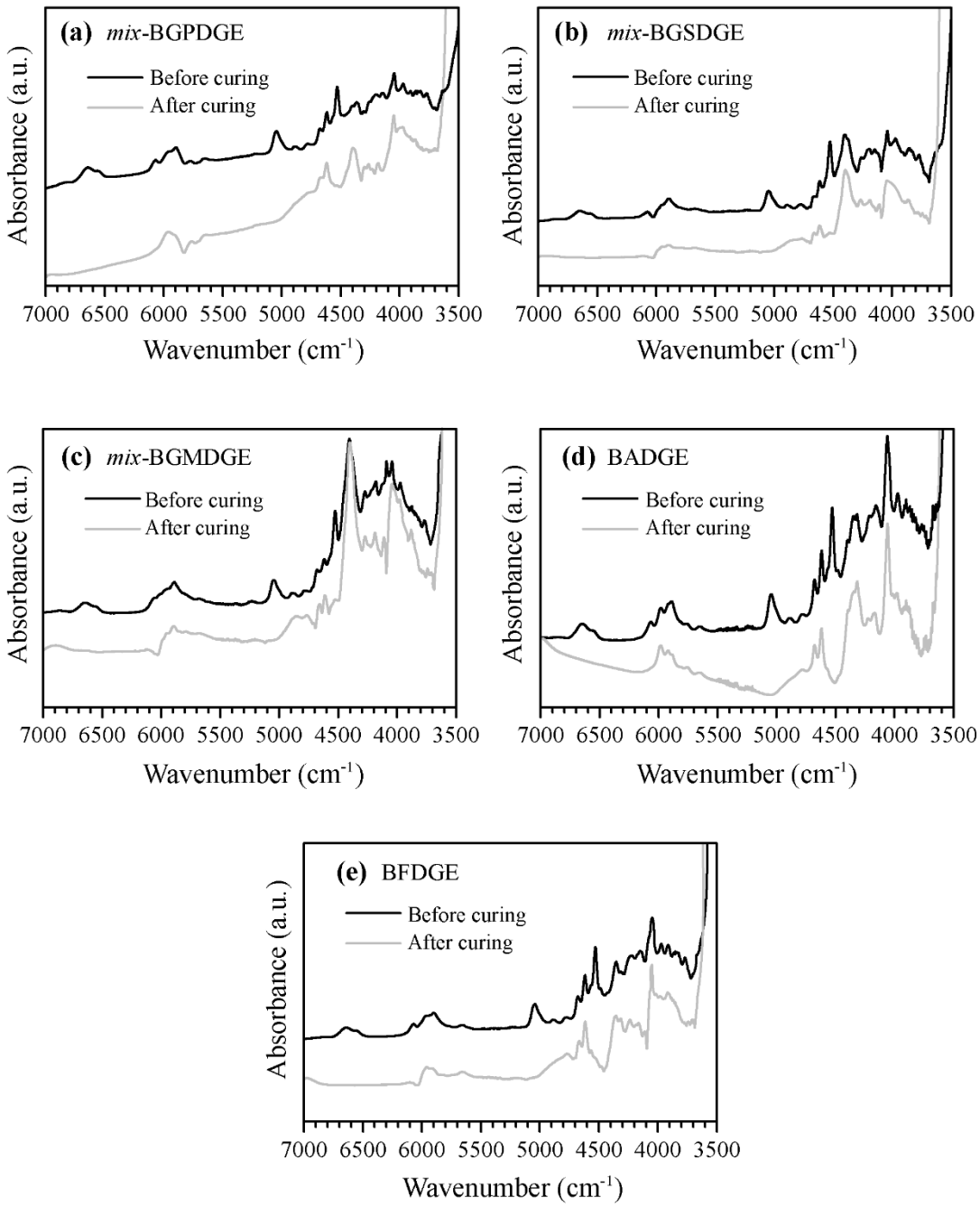

Figure S29. FTIR spectra before and after curing with MDA for (a) *mix*-BGPDGE, (b) *mix*-BGSDGE, (c) *mix*-BGMDGE, (d) BADGE, and (e) BFDGE. Near full conversion was confirmed qualitatively by the disappearance of the oxirane peak at 4530 cm^{-1}, the primary amine stretching peak at 5056 cm^{-1}, and the primary and secondary amine stretching peaks around 6670 cm^{-1}. Spectra were offset vertically for clarity.

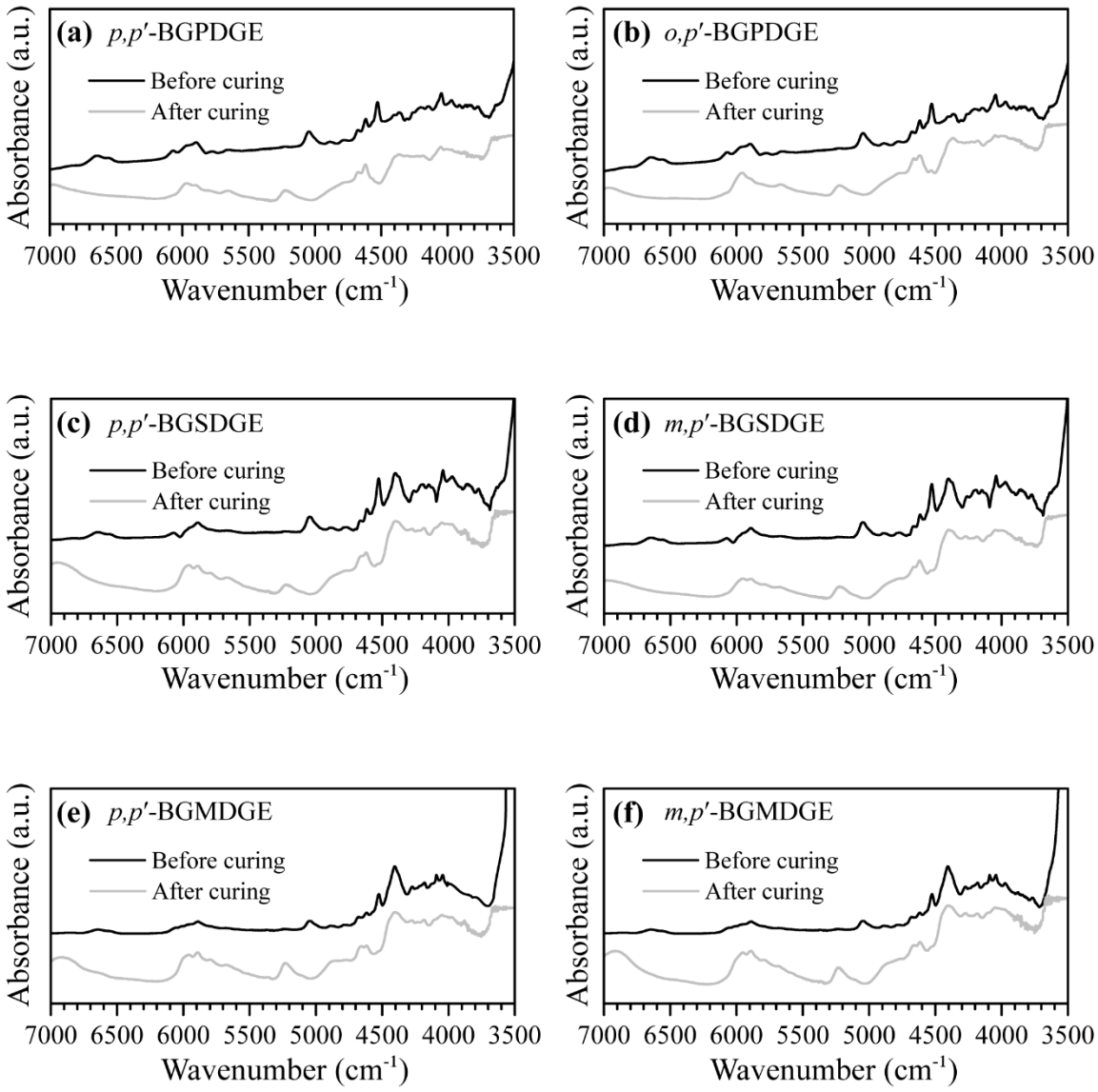

Figure S30. FTIR spectra before and after curing with MDA for (a) *p,p′*-BGPDGE, (b) *o,p′*-BGPDGE, (c) *p,p′*-BGSDGE, (d) *m,p′*-BGSDGE, (e) *p,p′*-BGMDGE, and (f) *m,p′*-BGMDGE. Near full conversion was confirmed qualitatively by the disappearance of the oxirane peak at 4530 cm^{-1}, the primary amine stretching peak at 5056 cm^{-1}, and the primary and secondary amine stretching peaks around 6670 cm^{-1} in the near IR region. Spectra were offset vertically for clarity.

Sample preparation for tensile testing

All pure regioisomer bisguaiacol diglycidyl ethers, BADGE, and BFDGE samples were prepared using the same protocol as samples for DMA and TGA testing except samples were cured in reusable dog bone shaped molds made in-house from silicone rubber and *n*-butyldimethylchlorosilane functionalized glass slides.[4] Samples with the dimensions provided in Scheme S1 were cured in air at 80 °C for 1 h, then 100 °C for 1 h, and subsequently postcured at 170 °C for 1 h.

Scheme S1. Dimensions of cured diglycidyl ether samples used for tensile testing.

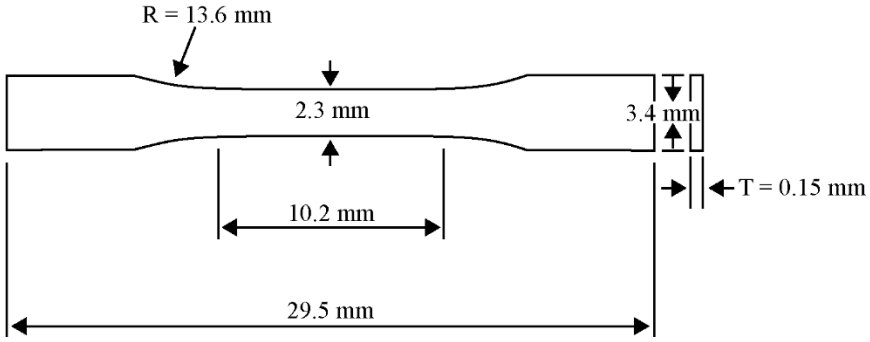

Tensile testing

Tensile testing was conducted on a Discovery Series Hybrid Rheometer (DHR, TA Instruments) using a film tension clamp, in tension mode at room temperature with a preload force of 0.1 N at a constant strain rate of 16 μm/s.

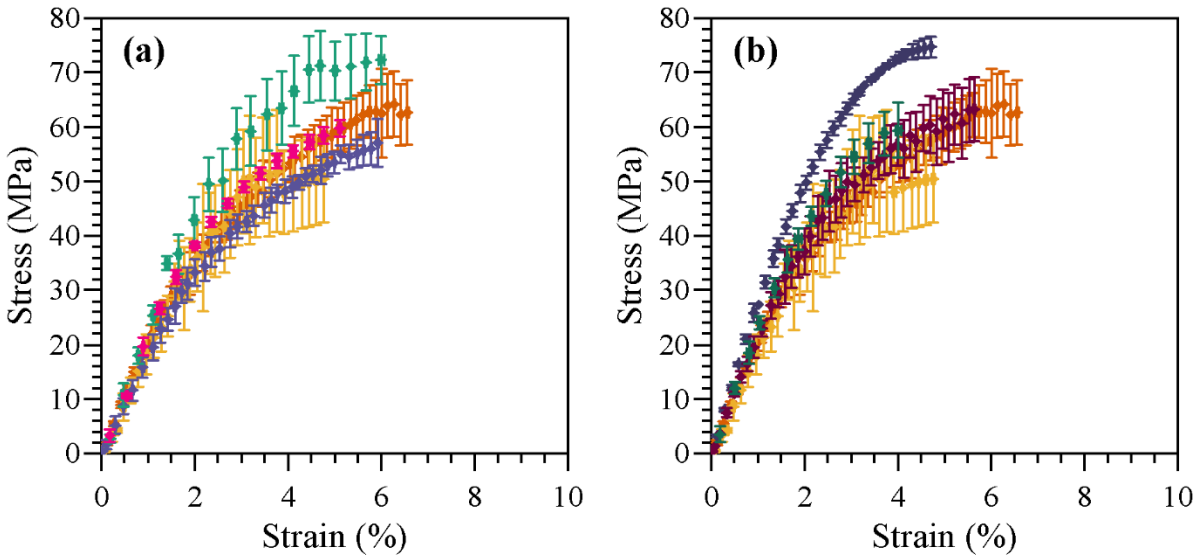

Figure S31. Stress-strain behavior of MDA cured (a) *p,p′*-BGPDGE (◆), *p,p′* BGSDGE (◆), *p,p′*-BGMDGE (◆), BADGE (◆), and BFDGE (◆) and (b) *o,p′*-BGPDGE (◆), *m,p′*-BGSDGE (◆), and *m,p′*-BGMDGE (◆) at a constant strain rate of 16 μm/s at room temperature.

Table S4. Fracture strain for cured pure regioisomer bisguaiacol diglycidyl ethers, BADGE, and BFDGE

Sample	Fracture strain (%)
p,p′-BGPDGE	7 ± 2
o,p′-BGPDGE	5 ± 2
p,p′-BGSDGE	6.1 ± 0.8
m,p′-BGSDGE	4.2 ± 0.4
p,p′-BGMDGE	8 ± 2
m,p′-BGMDGE	5.3 ± 0.5
BADGE	6.2 ± 0.5
BFDGE	5 ± 1

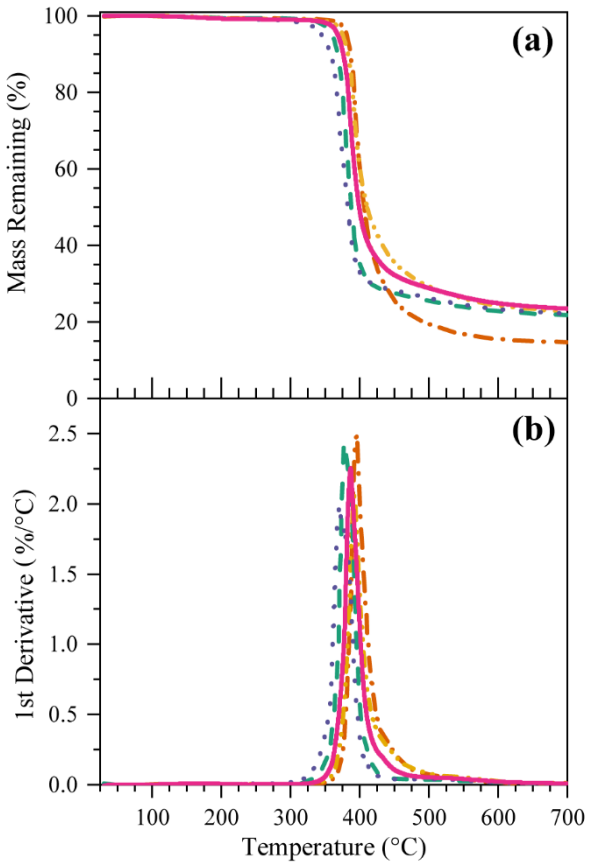

Figure S32. Full TGA thermograms of MDA cured *mix*-BGPDGE (———), *mix*-BGSDGE (– – –), *mix*-BGMDGE (· · · ·), BADGE (—·—·—), and BFDGE (—··—). (a) Sample mass remaining (%) as a function of temperature and (b) the first derivative of the sample mass remaining (%/°C) with respect to temperature in N_2 (50 mL/min) at a heating rate of 10 °C/min.

References

1. Lee, W. I.; Loos, A. C.; Springer, G. S., Heat of Reaction, Degree of Cure, and Viscosity of Hercules 3501-6 Resin. *J. of Compos. Mater.* **1982,** *16* (6), 510-520.
2. Montserrat, S.; Malek, J., A Kinetic Analysis of the Curing Reaction of an Epoxy Resin. *Thermochim. Acta* **1993,** *228*, 47-60.
3. Mijović, J.; Andjelić, S.; Kenny, J. M., *In situ* Real-time Monitoring of Epoxy/Amine Kinetics by Remote Near Infrared Spectroscopy. *Polym. Adv. Technol.* **1996,** *7* (1), 1-16.
4. Shelton, C. K.; Epps, T. H., III, Decoupling Substrate Surface Interactions in Block Polymer Thin Film Self-Assembly. *Macromolecules* **2015,** *48* (13), 4572-4580.